



Research paper

Design and characterisation of the out-of-plane dielectric elastomer generator for wave energy harvesting

Xi Wang ^a, Jinxin Wang ^a, Tianyou Zhang ^a, Jung-Che Chang ^a, Siqian Li ^a, Yao Zhang ^b, Tianyi Zeng ^a, Xin Dong ^{a,*}

^a Rolls-Royce University Technology Centre in Manufacturing and On-Wing Technology, Faculty of Engineering, University of Nottingham, NG7 2GX, Nottingham, UK

^b Department of Mechanical Engineering, University College London, WC1E 7JE, London, UK

ARTICLE INFO

Keywords:

Point absorber
Out-of-plane dielectric elastomer generator
Self-priming
Wave energy

ABSTRACT

Dielectric elastomers capable of converting mechanical energy into electrical energy have been extensively explored for wave energy harvesting. Among existing designs, a widely adopted approach involves a circular dome-shaped dielectric elastomer chamber, where air pressure between the water and the generator drives energy conversion. To enhance deployment feasibility, this paper proposes a novel point-absorber-inspired wave energy converter based on an out-of-plane dielectric elastomer generator (ODEG), which transforms linear mechanical motion into electrical energy through the buoy. A scaled-down prototype was designed and fabricated. The self-priming circuit was proposed for the ODEG to ensure continuous multi-cycle energy harvesting by autonomously replenishing the charge. This approach enabled efficiency to increase with cycle number and displacement amplitude. Furthermore, a constitutive model was developed to optimise the ODEG design and evaluate its energy conversion efficiency. The experimental investigation evaluated the performance of the ODEG under varying wave frequencies, amplitudes, and cycle numbers. The results demonstrated that the ODEG prototype was capable of harvesting wave energy across a frequency range of 0.1–1 Hz and a wave amplitude range of 30–50 mm. Specifically, the voltage boosted from 1.4 kV to 4.5 kV after 40 wave cycles at an amplitude of 50 mm.

1. Introduction

Wave energy, as a promising renewable resource, has attracted increasing attention as global energy demand continues to rise alongside growing concerns over environmental sustainability (Chen and Wu, 2024). One key area of research is the development of wave energy converters (WECs), which are designed to transform wave energy into electrical power (Aubry et al., 2011). Existing WEC systems employ a variety of energy conversion mechanisms, including electromechanical rotation (Xiao et al., 2021), hydraulic systems (Jusoh et al., 2019), piezoelectric effects (Renzi, 2016), dielectric elastomers (Moretti et al., 2020a, 2020c), and electromagnetic induction (Abu Husain et al., 2020). Among these, dielectric elastomer generators (DEGs), which employ soft-material-based approaches, feature a lightweight and simplified design. This results in a more favourable levelized cost of electricity (LCoE) compared to traditional mechanical WECs, which typically rely on substantial steel structures for energy conversion and

power generation.

To accommodate diverse application scenarios and harvest mechanical energy from various sources, DEGs have been developed in multiple structural configurations. The uniaxial-stretch planar configuration, which deforms along a single axis, offers a simple and scalable design. It is commonly employed in laboratory experiments to facilitate the study of DEG modelling and theoretical performance optimisation (Lv et al., 2015; Song et al., 2019). Similarly, the conical configuration primarily deforms axially and is well-suited for investigating energy harvesting efficiency due to its predictable deformation pattern (Bortot and Gei, 2015; Jiang et al., 2020). The cylindrical configuration enables a broader range of deformation modes, including axial elongation and bending, making it adaptable to a variety of application scenarios (Zhang, 2022). It has been applied in harvesting multidirectional, low-frequency sea wave energy (Vertechy et al., 2015), converting human motion into power for wearable and implantable devices (Fang et al., 2023), and capturing kinetic energy from fluid movements such as

* Corresponding author.

E-mail address: Xin.Dong@nottingham.ac.uk (X. Dong).

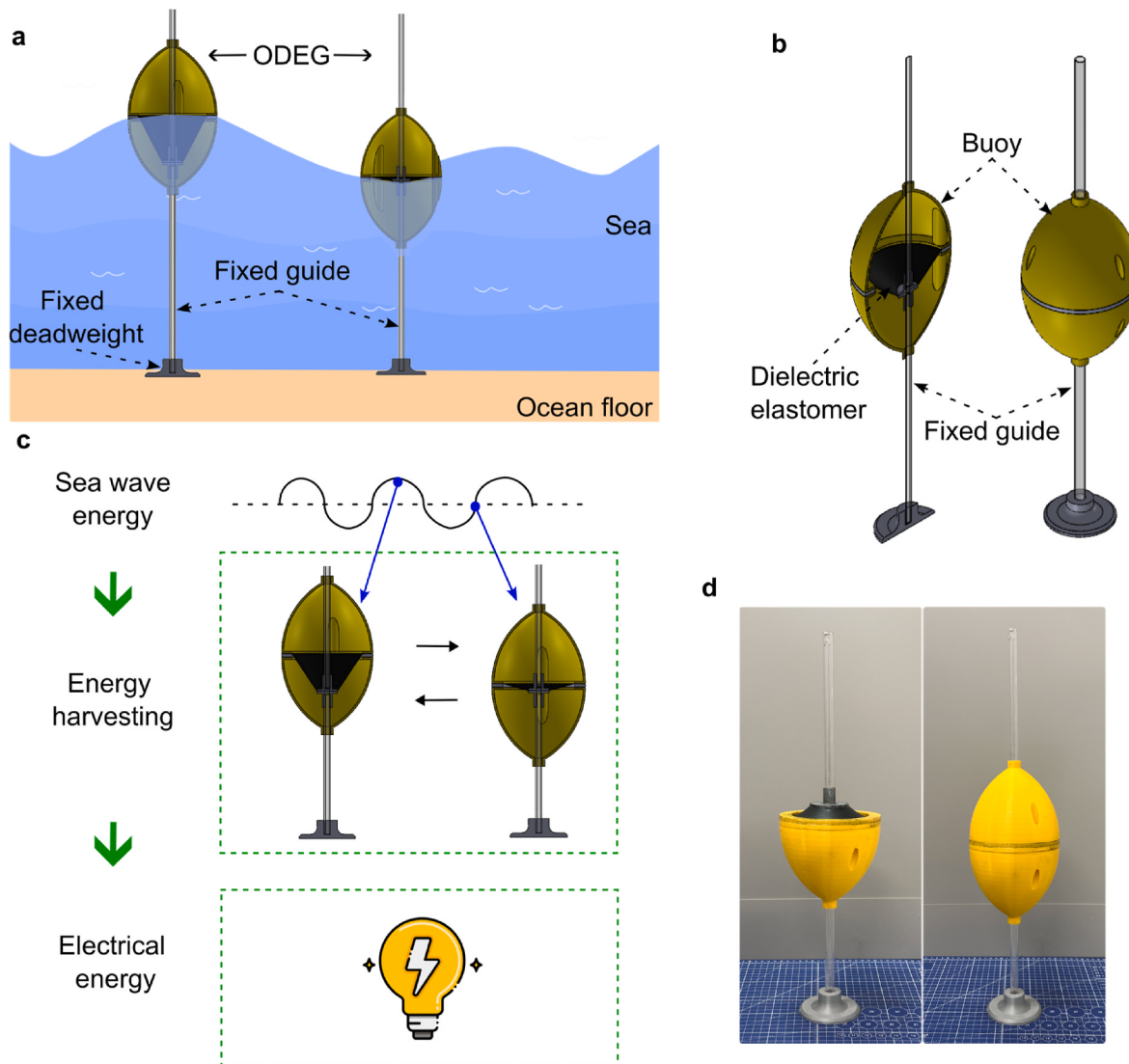


Fig. 1. ODEG prototype and application for harvesting wave energy. (a) Diagram of the ODEG deployed in the sea; (b) CAD modal of the ODEG; (c) Workflow of the ODEG convert the wave energy into electrical energy; (d) ODEG prototype (in Rolls-Royce University Technology Centre in Manufacturing and On-Wing Technology, University of Nottingham).

water currents and airflow.

In the ocean wave energy harvesting, the point-absorber is the most widely studied form (Moretti et al., 2020c). A typical device couples a primary hydrodynamic interface, which interacts with incoming waves and temporarily stores their potential energy for DEG that converts the captured mechanical motion into electricity. Two interface archetypes dominate current research, the one is floating-buoy configuration (Zeng and Wang, 2023), the buoy's oscillations are transmitted—via mechanical linkages—to an external DEG such as a multilayer stack (Lv et al., 2015), a planar uniaxial assembly (Binh and Ahn, 2016), or a diamond-shaped rotary unit (Moretti et al., 2015); however, the added linkages and moving parts can compromise reliability and scalability. By contrast, an oscillating-water-column (OWC) interface consists of a semi-submerged, hollow chamber partially filled with seawater, where wave-driven oscillations alternately compress and expand the trapped air pocket, thereby driving the generator (Falcão and Henriques, 2016). This type of the DEG forms a dome-shaped configuration (Moretti et al., 2019, 2020b), although the geometry offers a compact, compliant structure, its performance depends critically on wave-induced pressure: without sufficient pressure, the membrane only performs limited deformation, restricting energy capture across the broad range of

real-world sea states.

Various modelling approaches have been developed to enhance the understanding and prediction of the electromechanical behaviour of the DEG. Electromechanical coupled models describe the interaction between mechanical deformation, electrical charge distribution, and Maxwell stress, enabling the analysis of capacitance variations as a function of stretch (Moretti et al., 2019, 2020a). Finite Element Analysis (FEA) offers detailed simulations of large deformations, material nonlinearities, and electrode interactions, making it a critical tool for optimising device durability and efficiency (Cao et al., 2021; Srivastava and Basu, 2021). More recently, machine learning and AI-based modelling techniques have facilitated data-driven optimisation of DEG materials, structural designs, and operational strategies, further enhancing energy conversion efficiency (Medina et al., 2024).

To enable continuous energy harvesting, DEG require efficient power management circuits. Passive rectification circuits employ diodes to convert the AC-like output into DC power (Gurjar et al., 2025); however, they are often associated with voltage drop losses, which reduce efficiency. Active voltage-boosting circuits, such as switching regulators, enhance energy conversion efficiency by optimising charge transfer processes. Synchronous charge extraction techniques further improve

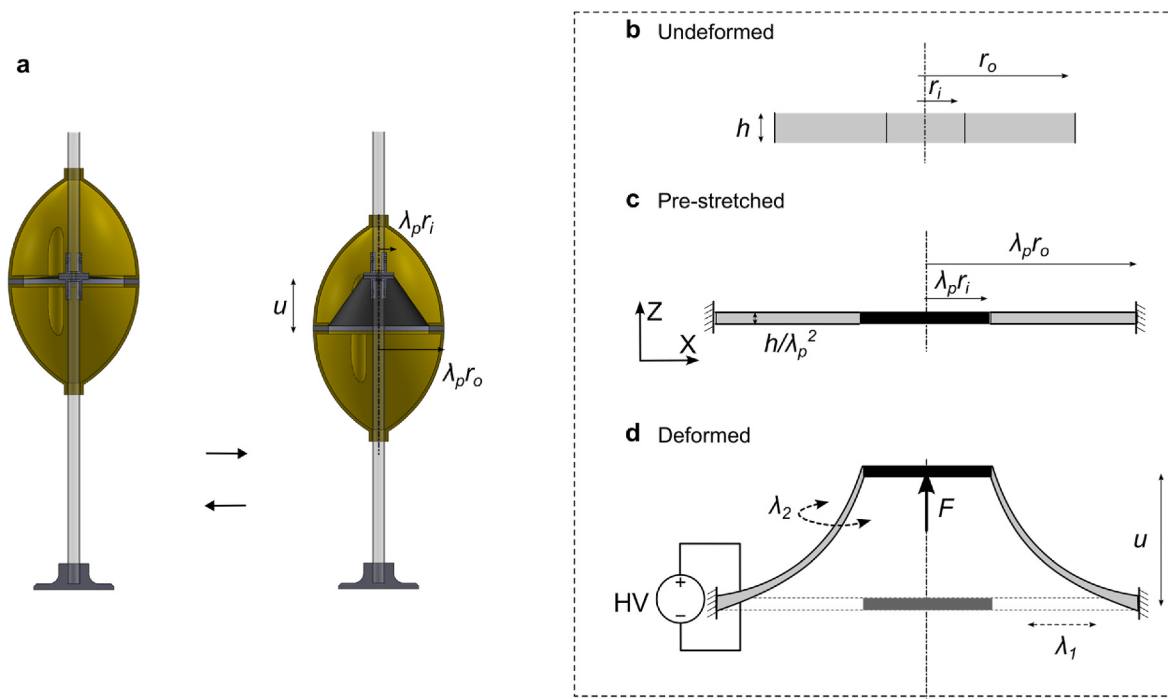


Fig. 2. Illustration of the ODEG pre-stretch and deformation. (a) Elastomer switch between pre-stretched and deformed state; (b) Undeformed elastomer (original state); (c) Elastomer pre-stretched and coated with the electrode while fixed by the inner and outer ring; (d) Elastomer is deformed out-of-plane by external force F .

performance by actively controlling the timing of charge transfer, thereby maximising energy extraction in each cycle. Additionally, hybrid storage solutions, integrating DEGs with supercapacitors or batteries, ensure a stable and continuous power supply, particularly for low-power electronic applications (Jean-Mistral et al., 2013). A key innovation in this field is the implementation of a self-priming circuit (Lai et al., 2023; McKay et al., 2010), which reduces energy losses during the charge-discharge cycle. It autonomously replenishes the charge on the DEG, enabling the DEG to operate with minimal external input and thereby enhancing the overall energy harvesting efficiency. Over the past two decades, self-priming circuits for DEGs have progressed from simple first-order topologies to sophisticated n -th-order designs tailored to specific operating conditions (Illenberger et al., 2016), with efforts to stabilise the voltage-boost performance. The latest advance is the integrated self-priming circuit (Illenberger et al., 2020), in which the entire circuitry is embedded directly within the dielectric membrane, creating a compact, application-ready solution.

Building on recent advances in dielectric-elastomer generators (DEGs), this study proposes a novel out-of-plane DEG (ODEG) for wave-energy harvesting. Drawing inspiration from the buoy-based point-absorber (Ji et al., 2021) architecture of the CorPower converter—which adapts to a broad spectrum of wave amplitudes and wavelengths (De Marinis, 2024; Zhou, 2016)—the novel design replaces its intricate electromechanical drivetrain with a compact, conical-membrane DEG. The buoy's vertical movement directly actuates the conical elastomer, inducing large out-of-plane displacement that are converted into electricity. This integration delivers two principal benefits over both traditional electromechanical and existing DEG-based point absorbers: (i) enhanced adaptability to diverse sea wave condition, inherited from the buoy dynamics, and (ii) integrating the conical shape DEG into buoy resulting a simplified architecture that streamlines fabrication, deployment, and maintenance. A theoretical model based on the Gent hyperelastic model is established to characterise the nonlinear mechanical behaviour of the elastomer under large deformations. Additionally, a self-priming circuit is integrated to enable continuous multi-cycle energy harvesting, enhancing the practical feasibility of

ODEG systems for marine applications. Laboratory experiments are conducted to evaluate the ODEG's performance under varying frequencies, displacement amplitudes, and cycle numbers, demonstrating its potential for efficient wave energy conversion.

2. ODEG for wave energy harvesting

Inspired by the point absorber wave energy converter, which regulates the cyclical sea wave into linear movement through the buoy and further transferred to the electrical energy, Fig. 1a and b presents a novel design and deployment of the out-of-plane dielectric elastomer generator (ODEG), a wave energy converter installed on the ocean floor through the fixed deadweight and guide, which harvests wave energy by converting the linear motion of the buoy into electrical energy through membrane deformation (Fig. 1c). To systematically investigate the energy harvesting performance of the ODEG, a scaled-down prototype was constructed, as illustrated in Fig. 1d. The ODEG consists of a dielectric elastomer ring with one end fixed to a guide stabilised on the deadweight and the other connected to an oval buoy. The oval buoy moves up and down in response to sea wave-induced buoyancy, cyclically deforming and relaxing the dielectric elastomer, thereby converting mechanical energy into electrical energy. To build the prototype, the VHB 4910 (3M) was used as dielectric elastomer, which can undergo elongation up to ten times its original length. The electrodes were made of carbon grease (846, MG Chemicals), ensuring good conductivity even under large stretching. The buoy, deadweight base, and additional fixtures were 3D-printed using PLA material (Ultimaker 2+).

3. Model of the ODEG

3.1. ODEG constitutive model

The ODEG is constructed with conical dielectric elastomer that able to go through out-of-plane deformation (Fig. 2a). Initially, the elastomer is stress-free and undeformed (Fig. 2b), with an original thickness h , an inner radius r_i , and an outer radius r_o . It is then subjected to a uniform

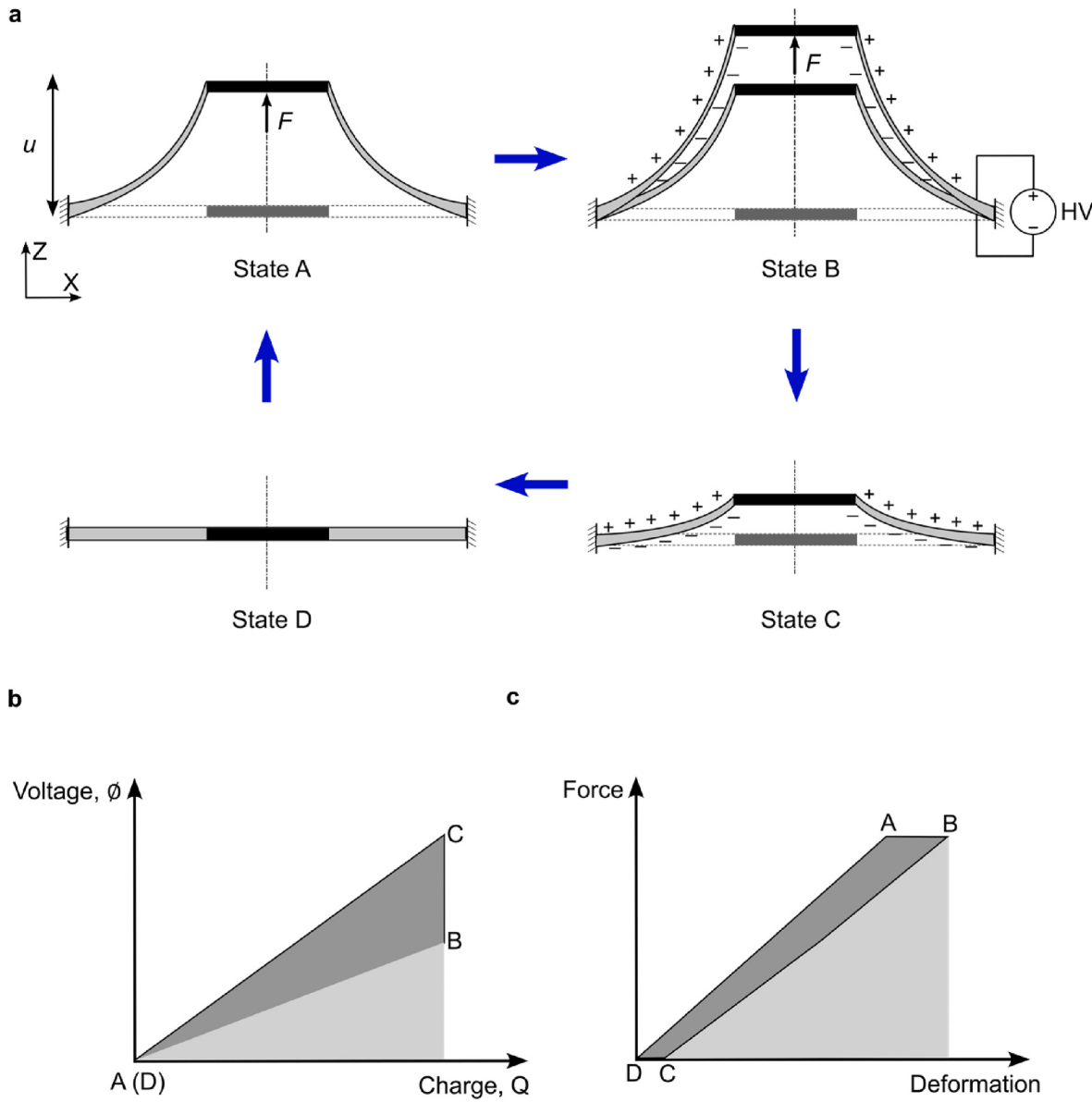


Fig. 3. Energy harvest cycle of the ODEG. (a) Four states of the ODEG configuration in one harvest cycle; (b) One harvest cycle in voltage-charge plane; (c) One harvest cycle in force-deformation plane.

Table 1
Physical parameters to build the ODEG prototype.

$\lambda_p r_o$	50 mm
$\lambda_p r_i$	25 mm
h	1 mm
λ_p	3
μ_1	17000 kPa
J_1	155
ε	4.5

radial pre-stretch by a factor of λ_p (Fig. 2c), and its outer boundary is fixed to a rigid ring with radius $\lambda_p r_o$, while its inner boundary is attached to a rigid circular plate with radius $\lambda_p r_i$. Subsequently, both surfaces are coated with a pair of compliant electrodes. By applying an external force F , the circular plate moves out of the plane relative to the outer ring (Fig. 2d).

As the elastomer is circular, the elastomer deformation is calculated

by radial strain (λ_1) and circular strain (λ_2). The elastomer layer is described as an incompressible hyperelastic material. Therefore, the elastomer layer deformation follows the relationship $\lambda_1 \lambda_2 \lambda_3 = 1$ (λ_3 is the strain of the elastomer in thickness). In the pre-stretched state, the elastomer strain is described as Fig. 2c, in the deformed state, the elastomer strain is described in Fig. 2d as the following equation (u is the displacement out-of-plane):

$$\lambda_1 = \lambda_p \sqrt{1 + \frac{u^2}{(r_o - r_i)^2}} \quad (1)$$

$$\lambda_2 = \lambda_p \quad (2)$$

Based on the Gent model (Gu et al., 2017; Wang et al., 2024a, 2024b), the energy density of the elastomer during the deformation can be represented as

$$W_s(\lambda_1, \lambda_2) = -\frac{1}{2} \mu_1 J_1 \ln \left(1 - \frac{\lambda_1^2 + \lambda_2^2 + \lambda_1^{-2} \lambda_2^{-2} - 3}{J_1} \right) \quad (3)$$

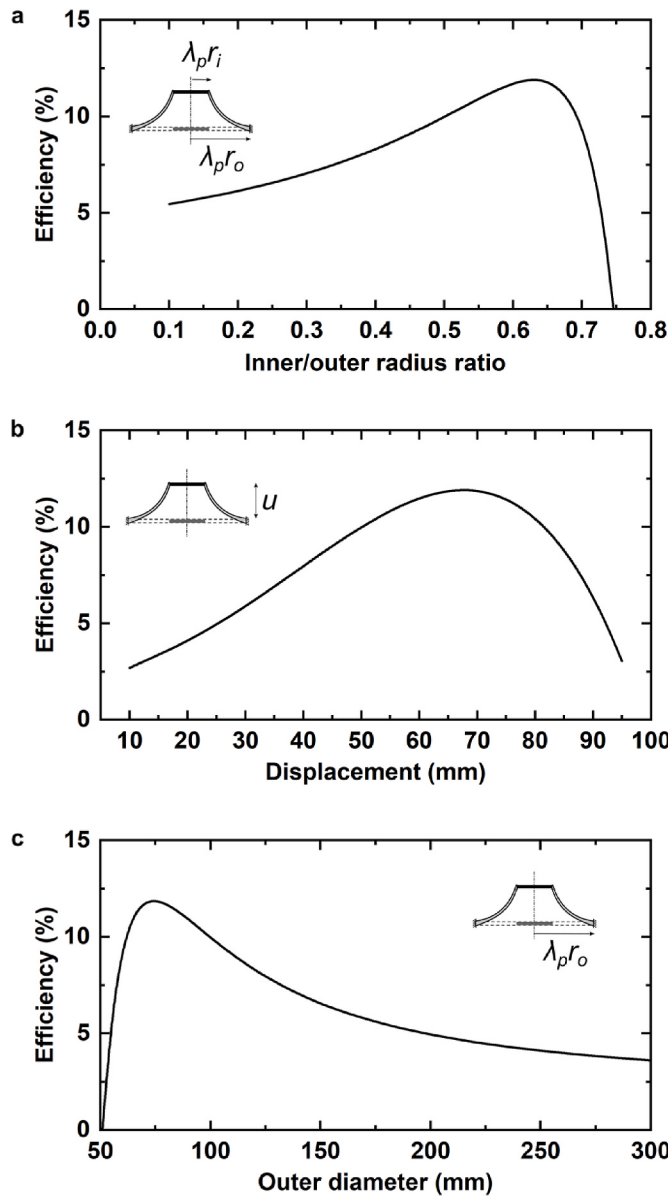


Fig. 4. Optimisation of the ODEG. (a) Efficiency vs inner/outer radius ratio, (displacement 50 mm; outer diameter 100 mm); (b) Efficiency vs displacement, (inner/outer radius ratio 0.5; outer diameter 100 mm); (c) Efficiency vs outer diameter, (inner/outer radius ratio 0.5; displacement 50 mm).

where μ_1 and J_1 are the shear modulus and the stretch limit of the elastomer. When the voltage is applied to the elastomer, the energy density of the elastomer is

$$W(\lambda_1, \lambda_2, D) = W_s(\lambda_1, \lambda_2) + \frac{D^2}{2\varepsilon} \quad (4)$$

where $\frac{D^2}{2\varepsilon}$ is associated with the external voltage, \emptyset is the applied voltage, Q is the electric charge on both electrodes, which can be further expressed as $Q = \varepsilon \frac{\emptyset}{h\lambda_3} A$, ε is the permittivity of the dielectric elastomer, defined as $\varepsilon = D/E$ with $D = Q/A$ and $E = \emptyset/h\lambda_3$. A is the area of the deformed elastomer $A = \pi\lambda_1(r_o^2 - r_i^2)$. Therefore, the charge on the elastomer is expressed as:

$$Q = \varepsilon \emptyset \lambda_1^2 \lambda_2 \pi (r_o^2 - r_i^2) \quad (5)$$

The stress in radial (λ_1) and circular (λ_2) direction are:

$$\sigma_1 = \mu_1 \frac{\lambda_1^2 - \lambda_1^{-2} \lambda_2^{-2}}{1 - \frac{\lambda_1^2 + \lambda_2^2 + \lambda_1^{-2} \lambda_2^{-2} - 3}{J_1}} - \varepsilon E^2 \quad (6)$$

$$\sigma_2 = \mu_1 \frac{\lambda_2^2 - \lambda_1^{-2} \lambda_2^{-2}}{1 - \frac{\lambda_1^2 + \lambda_2^2 + \lambda_1^{-2} \lambda_2^{-2} - 3}{J_1}} - \varepsilon E^2 \quad (7)$$

The external force to deform the elastomer out-of-plane is

$$F = \frac{\pi h}{\lambda_1 \lambda_2} (r_o + r_i) \left(\mu_1 \frac{\lambda_1^2 - \lambda_1^{-2} \lambda_2^{-2}}{1 - \frac{\lambda_1^2 + \lambda_2^2 + \lambda_1^{-2} \lambda_2^{-2} - 3}{J_1}} - \varepsilon E^2 \right) \sqrt{\frac{u}{u^2 + (r_o - r_i)^2}} \quad (8)$$

3.2. Energy harvesting analysis of the ODEG

As illustrated in Fig. 3a, the energy harvesting of the ODEG during one cycle can be described as four states: State A: deform the ODEG by a load F ; State B: charge the ODEG; State C: remove the load F and relax the deformation; State D: the charge is harvested and the ODEG recover to flat configuration. During this process, the mechanical energy is transformed to the electrical energy in State B and C, the harvested energy representation in voltage-charge plane and force-deformation plane are shown in Fig. 3b and c.

During one cycle energy harvesting (period T), the input mechanical energy can be calculated through

$$W_m = \int_0^T F(t) u'(t) dt \quad (9)$$

The harvested energy in one cycle is

$$W_{eh} = \frac{1}{2} (C_C \emptyset_C^2 - C_B \emptyset_B^2) \quad (10)$$

where $W_{eh} = \frac{1}{2} C_B \emptyset_B^2$ is the input electrical energy in one cycle. Using ratio $\beta = C_B/C_C$ to calculate the swing of the capacitance between state B and state C, which corresponds to the ODEG deformed between the loading and unloading state. The capacitance can be calculated as $C_C = \varepsilon \lambda_p^2 \pi (r_o^2 - r_i^2)/h$. Therefore, the harvested energy also can be expressed as

$$W_{eh} = \frac{1}{2} C_C \emptyset_B^2 (\beta^2 - \beta) \quad (11)$$

The efficiency of the energy harvesting in one cycle is

$$\eta = \frac{W_{eh}}{W_m + W_{ei}} \quad (12)$$

The influence of key geometric parameters on the energy-harvesting efficiency of the ODEG was calculated, using the dimension listed in Table 1 and the results were presented in Fig. 4. Three factors were investigated: (i) Inner-to-outer radius ratio, this ratio sets the active membrane area, the optimised range is between 0.5 and 0.7, within the range the theoretical efficiency reach up to 12%; (ii) Displacement, it indicates the external wave amplitude, which exhibits an optimum between 50 mm and 80 mm; (iii) Outer diameter, governing the overall device dimension, the most effective value is between 80 mm and 120 mm. Together, these findings provide the guideline to design the optimised ODEG either large scale prototype for the real ocean test or small scale prototype for laboratory test.

4. Self-priming circuit for ODEG

As shown in Fig. 3a, the fundamental energy harvesting process of the ODEG requires an external charge supply in each cycle. While this is feasible for laboratory testing, it poses a significant challenge for practical applications. Furthermore, charge leakage and consumption by the electrical load lead to charge loss over time. Without periodic

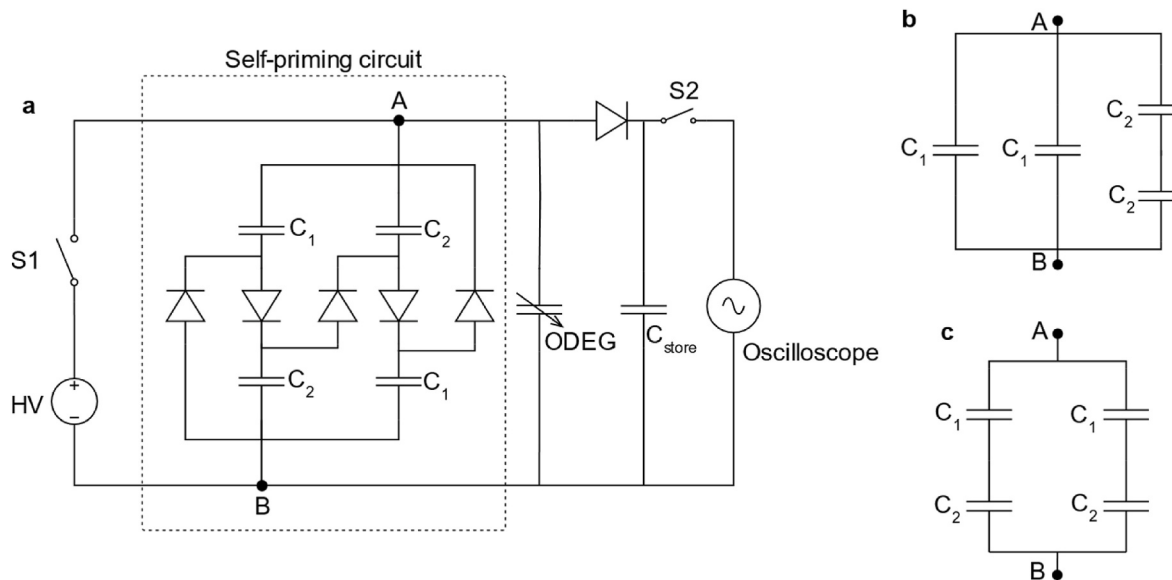


Fig. 5. A schematic of the electrical system used in the experiments. (a) Diagram of the circuit for energy harvest; (b) Self-priming circuit in high charge state (between node A and B); (c) Self-priming circuit in high voltage state (between node A and B).

replenishment, the charge on the ODEG will gradually dissipate. Therefore, a self-priming circuit is crucial for ODEG intended for real-world applications.

Fig. 5a depicts the electrical system, which consists of a power source (DC power supply and high voltage converter, XP power, Q101-5), a two-order self-priming circuit, the ODEG, and an oscilloscope (Tektronix, TBS2000B). The two-order self-priming circuit is composed of four capacitors and five high-voltage diodes, functioning collaboratively to regulate current flow and autonomously replenish charge losses without relying on an external power source on every cycle (McKay et al., 2010). The charge transfer process involves four key phases:

Phase i: ODEG deformation (Capacitance increases). During deformation, the capacitance of the ODEG increases. At this stage, no current flows from the self-priming circuit to the ODEG because the voltage across the ODEG is higher than the circuit voltage.

Phase ii: Charge transfer from the self-priming circuit to the ODEG. As the deformation progresses, the voltage across the ODEG decreases below the circuit voltage. This potential difference drives current from the self-priming circuit into the ODEG, slowing the voltage drop and replenishing the charge. In this high-charge phase, the capacitors in the self-priming circuit are connected in parallel (Fig. 5b).

Phase iii: ODEG relaxation (Capacitance decreases). As the ODEG relaxes, its capacitance decreases. No current flows back to the self-priming circuit because the voltage across the circuit exceeds that of the ODEG.

Phase iv: Charge transfer from the ODEG to the self-priming circuit. With continued relaxation, the voltage across the ODEG increases above the self-priming circuit voltage. This drives current from the ODEG back into the self-priming circuit, boosting the circuit voltage. During this high-voltage phase, the capacitors in the self-priming circuit are configured in series (Fig. 5c).

To ensure efficient charge transfer, the proportional voltage swing across the ODEG should exceed the voltage difference between the two states of the self-priming circuit.

5. Experiment and result

In this section, the mechanical properties and energy harvesting performance of the ODEG are investigated experimentally. Firstly, the force-deformation behaviour of the ODEG is examined to understand its mechanical response under external loading. Next, the energy

harvesting performance over a single cycle is tested and compared with calculation result under varying deformation amplitudes and frequencies. Finally, the voltage boosting effect and energy harvesting capability of the ODEG during multi-cycle operations, incorporating a self-priming circuit, are evaluated experimentally. During the experiments, the ODEG is driven at input frequencies of 0.1–1 Hz, matching real ocean-wave conditions (De Marinis, 2024; Jiang et al., 2023; Viet and Wang, 2018). The excitation displacement ranges between 30 mm and 50 mm. Because the ODEG tested here is a scaled-down prototype, a scaling-up analysis for a full-scale device is performed in Section 7. This analysis predicts the performance of the up-scaled ODEG when deployed in a real-ocean environment characterised by 4.5 m-high waves, aligning with the actual ocean-wave amplitude.

5.1. Experiment setup

Fig. 6a shows the experimental setup for testing the force-deformation mechanical properties of the ODEG. In this setup, the ODEG buoy is securely held in place by a fixture, while the guide, connected to both a load cell (LCFD-1KG, Omega) and a motor (DC motor, Maxon), measures the force corresponding to the applied deformation. Similarly, Fig. 6b depicts the excitation setup for ODEG to evaluate its energy harvesting performance. A stepper motor coupled with a linkage mechanism generates a sea wave-like excitation. The ODEG buoy is fixed using a fixture, while the motor provides external excitation with adjustable frequency, amplitude, and initial voltage.

Fig. 7 presents the exploded view of the ODEG. The outer side of the pre-stretched elastomer, which is sandwiched between electrodes, is bonded to the outer ring and further secured by the buoy. The inner side is attached to the inner ring and stabilised by the fixed guide. A piece of copper is affixed to the inner surface of the electrode and held in place by the inner ring. This copper strip is electrically connected to the self-priming circuit (as shown in Fig. 5) via a wire that passes through the fixed guide.

5.2. Mechanical and electrical properties of the ODEG

This section investigates the mechanical and electrical properties of the ODEG built using the parameters shown in Table 1, specifically its response to external loading and the corresponding capacitance variations under different displacement amplitudes. Fig. 8a shows the

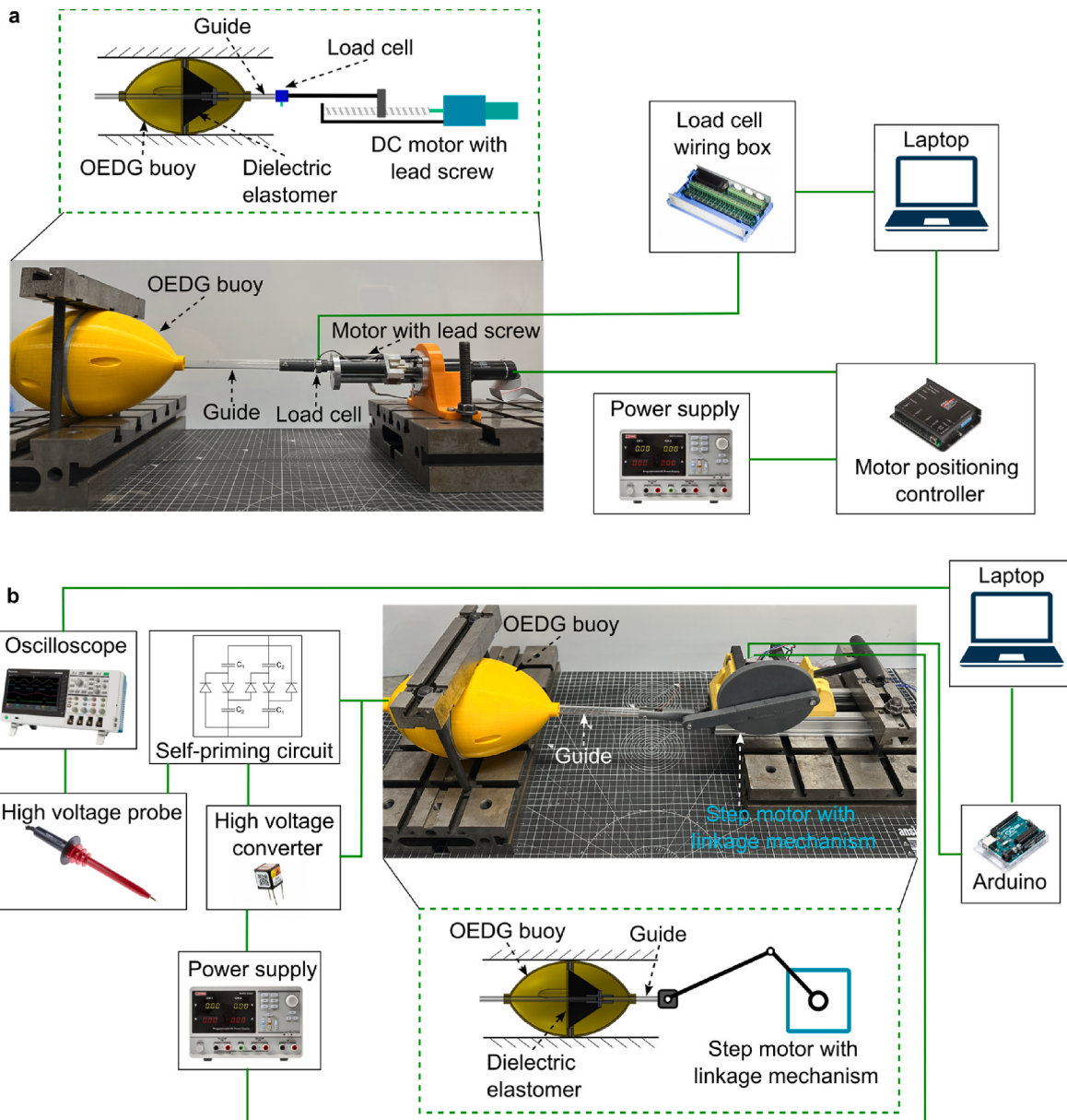


Fig. 6. Experiment setup. (a) Setup for force–deformation mechanical properties; (b) Excitation setup for evaluating energy harvesting performance.

calculated force-displacement behaviour, which is validated by experimental results. When the ODEG is deformed for 50 mm, the maximum reaction force reaches 13.4 N. Fig. 8b illustrates the ODEG's capacitance change during deformation. The initial capacitance is 2.11 nF in the flat state; this value doubles when the displacement reaches 28 mm. The maximum capacitance, achieved at 50 mm, is 10.56 nF, five times that of the initial configuration. To ensure efficient charge transfer, the proportional voltage swing across the ODEG should exceed the voltage difference between the two states of the self-priming circuit. Therefore, the working range of the self-priming circuit is estimated from 28 mm to 50 mm. Table 2 lists the specific capacitors used in the self-priming circuit.

5.3. Single-cycle energy harvest

To understand how the ODEG harvest the wave energy in a single cycle, i.e., State B to State C, as illustrated in Fig. 3a, the circuit, as

shown in Fig. 5a, is used to experimentally investigate the voltage boost and energy harvesting in a single cycle. The capacitance of the self-priming circuit, ODEG and the storage capacitor are represented by C_{sp} , C_B (C_C) and C_{store} , respectively, among them, the C_{sp_hv} (2.67 nF) is used to represent the self-priming high voltage state and used the C_{sp_hc} (6 nF) to represent the high charge state. Two switches are kept open at the beginning. The ODEG is initially charged with the start voltage ϕ_B by closing the switch S1 while it is deformed (State B). Then, the voltage is removed by closing the switch S1; the ODEG deformation is subsequently released (State C). The ODEG transfers the mechanical energy into electrical energy while boosting the initial voltage to a higher level and storing it in the capacitor C_{store} through the diode. Then, switch S2 is closed, allowing the oscilloscope to measure the boosted voltage of the capacitor C_{store} . In this experiment, the starting voltage ϕ_B (Voltage at State B) and the boosted voltage ϕ_C (Voltage at State C) were measured, their relation can be represented by $(C_{sp} + C_B + C_{store})\phi_B = (C_{sp} + C_C + C_{store})\phi_C$. Specifically, when the capacitance swing of the C_B exceeds the

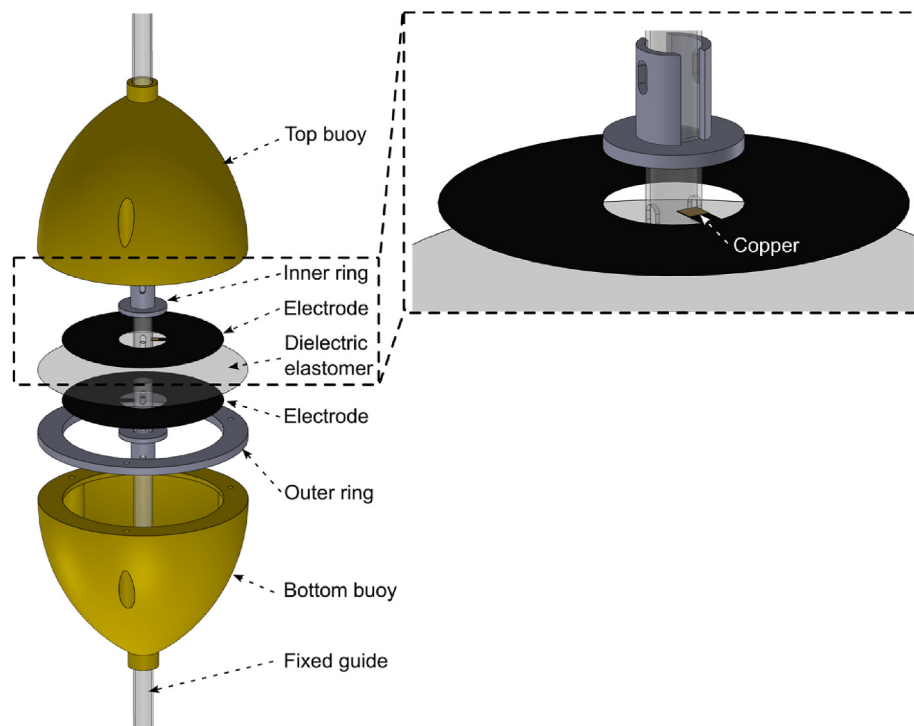


Fig. 7. Exploded view of the ODEG CAD model.

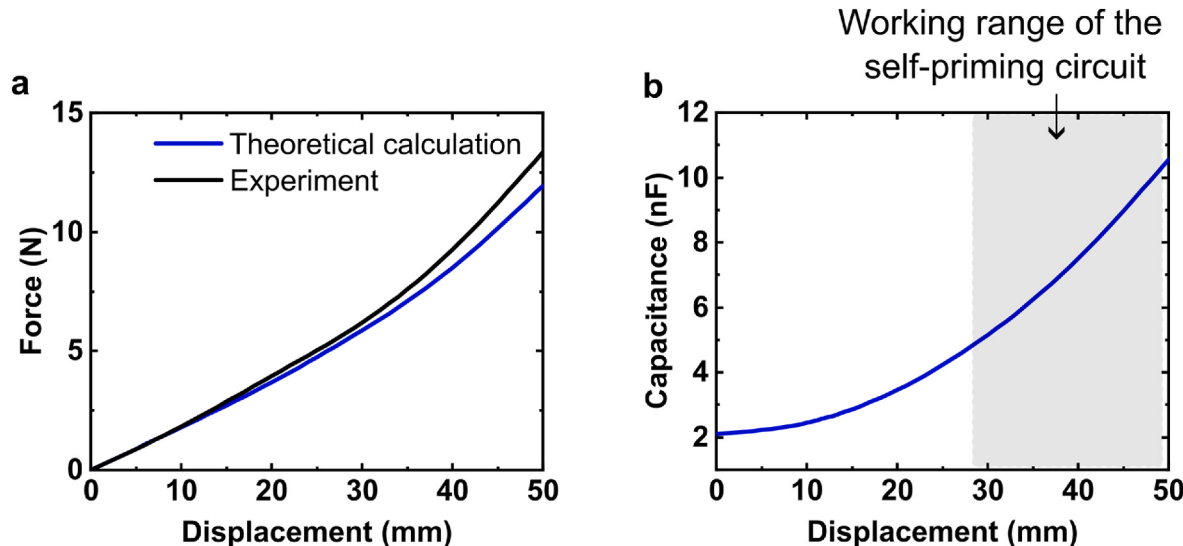


Fig. 8. Mechanical and Electrical Property of the ODEG. (a) Theoretical calculation and experiment of the force-displacement property of the ODEG (The calculation results are obtained from equation (8)); (b) Calculated capacitance of the ODEG in various displacements.

Table 2
Capacitors for the self-priming circuit.

C ₁	2 nF
C ₂	4 nF
C _{store}	4 nF

critical value $C_{B_critical}$ that triggers the self-priming circuit to switch between the high-voltage and high-charge states, the boosted voltage \mathcal{O}_C can be calculated by the following equation:

$$\mathcal{O}_C = \begin{cases} \frac{(C_{sp_hv} + (C_B - C_{B_critical}) + C_{store})}{(C_{sp_hv} + C_C + C_{store})} \mathcal{O}_B & (C_B > C_{B_critical}) \\ \frac{(C_B + C_{store})}{(C_C + C_{store})} \mathcal{O}_B & (C_B \leq C_{B_critical}) \end{cases} \quad (13)$$

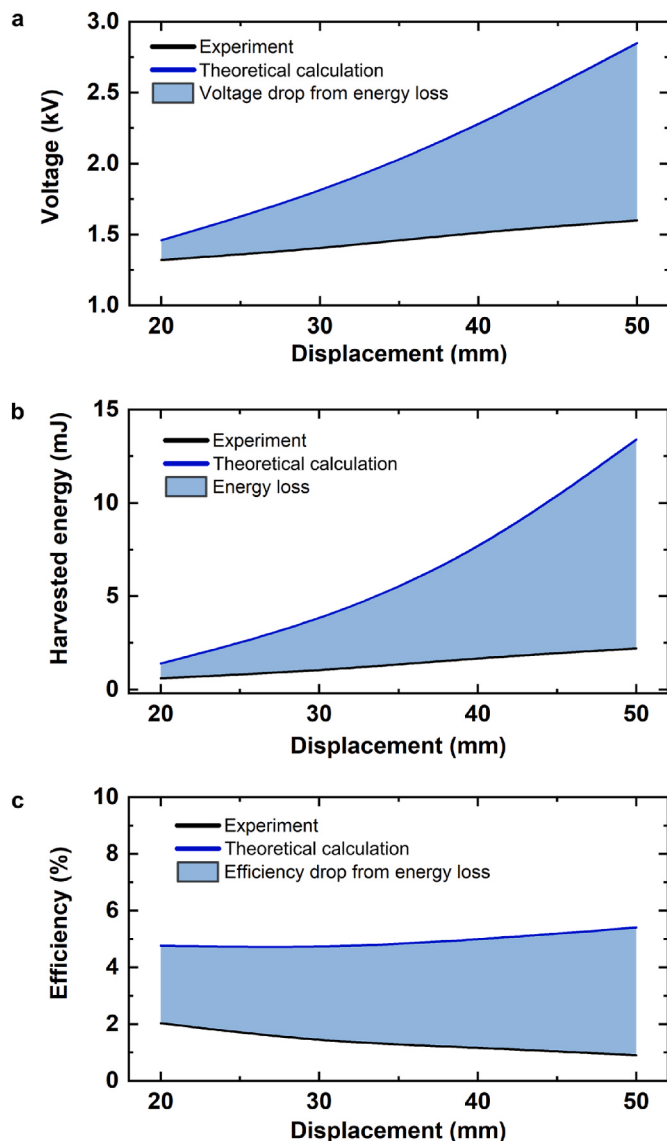


Fig. 9. Theoretical calculation and experimental results of ODEG energy harvesting in a single cycle (1Hz). (a) Voltage boost; (b) Harvested energy; (c) Efficiency (The calculation results are obtained from equations (13)–(16)).

$$C_{B_critical} = \frac{C_{sp_hc}}{C_{sp_hv}} C_C \quad (14)$$

The input energy and harvested energy stored to C_{store} are

$$W_{ei} = \frac{1}{2} C_{store} \emptyset_B^2 \quad (15)$$

$$W_{eh} = \frac{1}{2} C_{store} (\emptyset_C^2 - \emptyset_B^2) \quad (16)$$

According to the calculations presented in Equations 13–16, a larger-value storage capacitor results in a smaller voltage boost per cycle but offers better energy storage capacity. This makes it more suitable for field tests, where energy harvesting over a large number of cycles is desired. In contrast, a smaller-value storage capacitor produces a more visible voltage boost in a single cycle, but with lower overall energy storage capacity, making it more appropriate for laboratory testing.

Fig. 9 compares the calculated and experimental energy-harvesting metrics—voltage boost, harvested energy, and efficiency—recorded during a single 1 Hz cycle while the displacement is varied from 20 mm to 50 mm. Both the voltage boost and the harvested energy rise

monotonically with increasing displacement, whereas the efficiency remains constant throughout the tested range. The shaded band between the calculated and experimental data represents the energy loss, which have not been considered in the current model, originates from two sources. (i) Electrical dissipation (also reported in (McKay et al., 2014)). Charge leakage and joule losses in the circuit loop, including electrical component and elastomer electrode, the larger elastomer deformation results in larger resistance and thus the larger energy loss, as indicated in Fig. 9a and b. (ii) Viscoelastic damping (also reported in (McKay et al., 2010)). The inherent viscosity of the dielectric elastomer dissipates mechanical work during cyclic deformation, further reducing the recoverable electrical energy.

Fig. 10 further experimentally investigated the voltage boost and energy harvesting performance of the ODEG under different wave amplitudes and frequencies. The voltage boost results indicate that higher wave amplitudes and frequencies lead to a larger voltage boost. Specifically, the voltage can be boosted from 1.2 kV to 1.6 kV under a 50 mm displacement at 1 Hz. The frequency range selected for the experiment, from 0.1 Hz to 1 Hz, aligns with the typical wave frequencies observed at sea. Fig. 10b presents the corresponding harvested energy and efficiency under various amplitudes and frequencies. Similarly, larger displacement and higher frequency contribute to increased energy harvesting. With respect to efficiency, higher frequencies result in better efficiency, whereas the efficiency remains nearly constant across the displacement range from 20 mm to 50 mm. The experimental maximum efficiency is observed at 1 Hz, while the lower frequencies lead to reduced efficiency due to charge leakage, as discussed in Fig. 9.

5.4. Multi-cycle energy harvest with self-priming circuit

By employing a self-priming circuit to replenish the charge on the ODEG, it is able to achieve continuous wave energy harvesting, with the harvested energy stored in a storage capacitor. Therefore, the multi-cycle energy harvesting capability of the ODEG under periodic external excitation is investigated. In the experiment, the setup shown in Figs. 5a and 6b is used. In the beginning, both switches are kept open. Subsequently, switch S1 is closed to charge the entire circuit, including the self-priming circuit, the ODEG, and the storage capacitor, while the ODEG is in its flat configuration (State A). Once the charging process is complete, switch S1 is opened, and the ODEG is subjected to periodic excitation. After a specific number of excitation cycles, switch S2 is closed to measure the energy stored in the storage capacitor. Throughout the test, the initial voltage boosted voltage, and the number of cycles is recorded to evaluate the energy harvesting performance of the ODEG.

Fig. 11 presents the original oscilloscope data captured over a 10 s interval. At $t = 5$ s, switch S2 is closed, inserting the oscilloscope into the circuit to monitor the voltage across the storage capacitor. This action produces a sharp ramp-up, after which the voltage decays due to closed circuit; the instantaneous peak reached immediately after switch-on is taken as the boosted voltage. For reference, the dotted line plots the input voltage applied to the ODEG. Fig. 12 shows the experimental results of the multi-cycle voltage boost and energy harvesting performance of the ODEG. Theoretically, the voltage can be continuously boosted with increasing excitation cycles until the elastomer undergoes dielectric breakdown. To ensure the safety of the elastomer, the maximum voltage is kept below 5 kV throughout the experiments. The energy harvesting performance of the ODEG under various displacement amplitudes, frequencies, and initial voltages is investigated. As discussed in Section 4 and shown in Fig. 8b, the capacitance swing between the flat and deformed states should double to enable the self-priming circuit to replenish the charge on the ODEG. Therefore, 30 mm, 40 mm, and 50 mm displacement amplitudes are selected for the tests.

Fig. 12a shows the voltage boost performance with an initial voltage of 1.4 kV under a 1 Hz excitation and displacement amplitudes of 30 mm, 40 mm, and 50 mm. The results indicate that the voltage is boosted

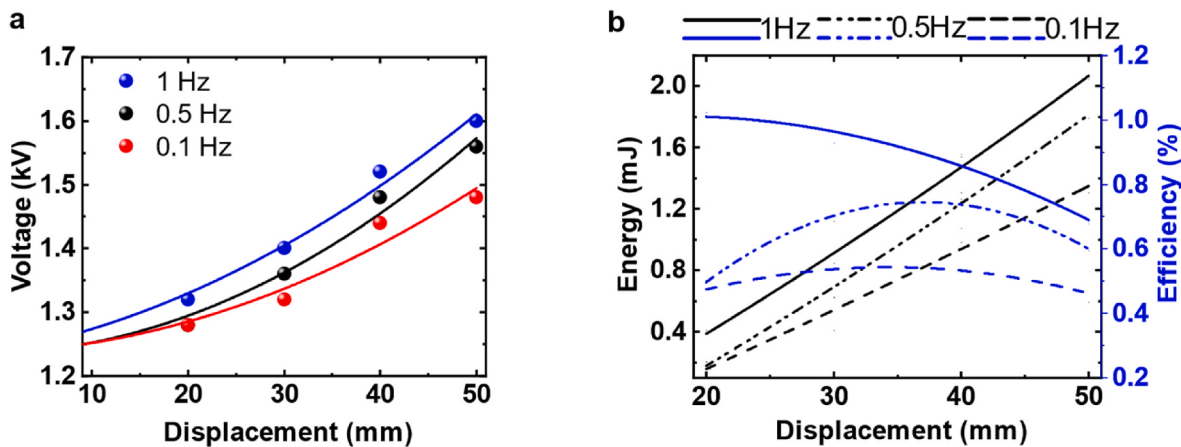


Fig. 10. Voltage boost and energy harvesting of the ODEG in a single cycle. (a) Voltage boost in different displacements and frequencies; (b) Harvested energy (represented in black) and efficiency (represented in blue) in different displacements and frequencies. (Note: the curves in the figure are second-order polynomial fit based on the experimental discrete points). (For interpretation of the references to colour in this figure legend, the reader is referred to the Web version of this article.)

from 1.4 kV to 4.5 kV after 40 cycles when the displacement amplitude is 50 mm. In comparison, it requires 60 cycles to reach the same voltage level with a displacement of 40 mm, and 110 cycles with a displacement of 30 mm. Fig. 12b presents the corresponding harvested energy and efficiency. The harvested energy exhibits a similar increasing trend to the voltage boost. The efficiency improves with the number of cycles due to the increasing voltage. Additionally, larger displacement amplitudes lead to higher efficiency. Further experiments are conducted to evaluate the multi-cycle energy harvesting performance under different frequencies, i.e., 0.1 Hz, 0.5 Hz, and 1 Hz, with a displacement amplitude of 40 mm and an initial voltage of 1.4 kV, as shown in Fig. 12c and d. The results demonstrate that higher frequencies result in better voltage boosting and larger efficiency. In Fig. 12e and f, the initial voltage is set to 1.36 kV, 1.48 kV, and 2.08 kV while keeping the frequency at 1 Hz and the displacement amplitude at 40 mm. The results are consistent with the observations in Fig. 12c and d, indicating that a higher initial voltage enhances both voltage boosting and efficiency.

6. Conclusion

Inspired by the wave energy point absorber, this paper presented a novel out-of-plane dielectric elastomer generator (ODEG) based wave energy harvesting prototype, integrating a self-priming circuit to enable autonomous charge replenishment. To evaluate the electromechanical performance of the ODEG, a constitutive model based on the Gent hyperelastic model was formulated. The implementation of a self-priming circuit proved essential in enabling continuous multi-cycle energy harvesting, significantly enhancing the practicality of ODEG systems for real-world marine applications. The experimental and theoretical investigations presented in this work demonstrate the potential of ODEG as an effective solution for wave energy harvesting. The results highlight that displacement amplitude and frequency strongly influence the voltage boost and harvested energy. Larger displacement amplitudes and higher frequencies lead to improved energy harvesting performance, while a higher initial voltage accelerates the voltage-boosting process during multi-cycle operations.

The Experimental test of the ODEG achieved a maximum voltage boost from 1.4 kV to 4.5 kV after 40 excitation cycles with a displacement amplitude of 50 mm and frequency of 1 Hz. The integration of the self-priming circuit enabled continuous multi-cycle energy harvesting, enabling efficiencies to increase with cycle number and displacement amplitude. However, the experimental results also reveal limitations. At lower frequencies, efficiency decreases due to charge leakage over extended periods.

7. Discussion and future work

The experimental results demonstrate that the out-of-plane dielectric elastomer generator (ODEG) is technically capable of functioning as a point absorber for harvesting ocean wave energy. To further evaluate its feasibility and performance in real-world ocean conditions, this work take the deployment of a commercial point absorber—CorPower C4—as a reference case (De Marinis, 2024). The ODEG is scaled up to match the dimensions of the CorPower C4 (buoy diameter: 9 m, height: 18 m, operational stroke range: 2.7–4.5 m), while maintaining a single elastomer layer thickness of 0.1 mm, resulting in a total thickness of 0.3 m (i.e., 3000 layers). Under a 0.1 Hz wave frequency with a 4.5 m stroke, the scaled-up ODEG is capable of harvesting 36.45 kJ of energy per cycle, corresponding to a device power ratio of 3645 W. This value could be further increased by stacking more elastomer layers. A key advantage of this approach is its structural simplicity—consisting solely of the buoy shell and the elastomer—which leads to a lightweight and low-cost system compared to conventional commercial point absorbers. One consideration for real-world deployment is electrical insulation. Since the elastomer operates under high voltage and is coated with compliant electrodes, an insulation layer is required to isolate the electrodes from the marine environment. Ideally, both the elastomer and the electronic components should be encapsulated within a low-modulus, highly stretchable silicone material to ensure reliable operation and durability in ocean conditions.

Future research will aim to enhance the performance and reliability of the current ODEG system. One direction is the improved model that considering the energy loss factor which can be used to predict and optimise the energy harvesting performance under time-varying wave signals. Another direction is the development of adaptive control strategies, including the implementation of real-time control algorithms to optimise the charging and discharging processes, as well as the power take-off (PTO) system. This approach is expected to improve energy conversion efficiency under varying sea conditions. Then is field testing (Sergienko et al., 2024) of the current ODEG prototype in real marine environments to assess its long-term operational stability and energy harvesting capability under actual wave conditions (Joensen and Birmingham, 2024). The harvested electrical energy can be collected by the power take-off system and used to power an LED, serving as a blinker for maritime navigation.

CRediT authorship contribution statement

Xi Wang: Writing – review & editing, Writing – original draft,

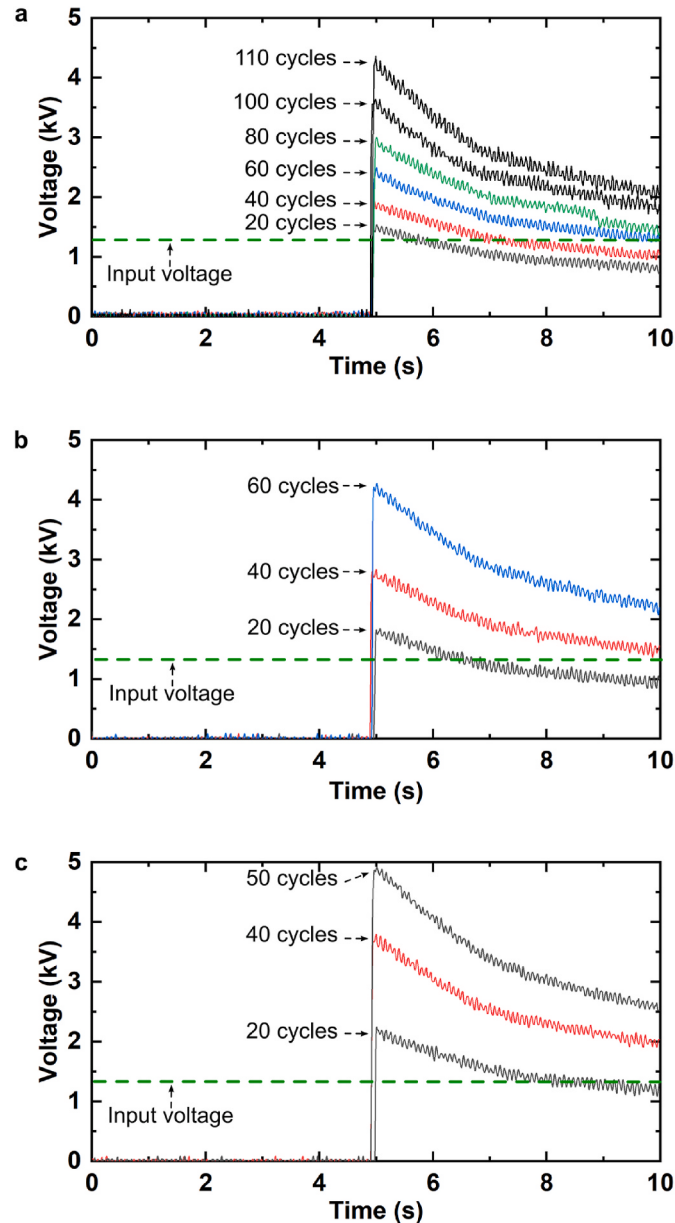


Fig. 11. Time domain original voltage boost data from oscilloscope (start voltage: 1.4 kV; frequency: 1Hz). (a) Displacement: 30 mm; (b) Displacement: 40 mm; (c) Displacement: 50 mm.

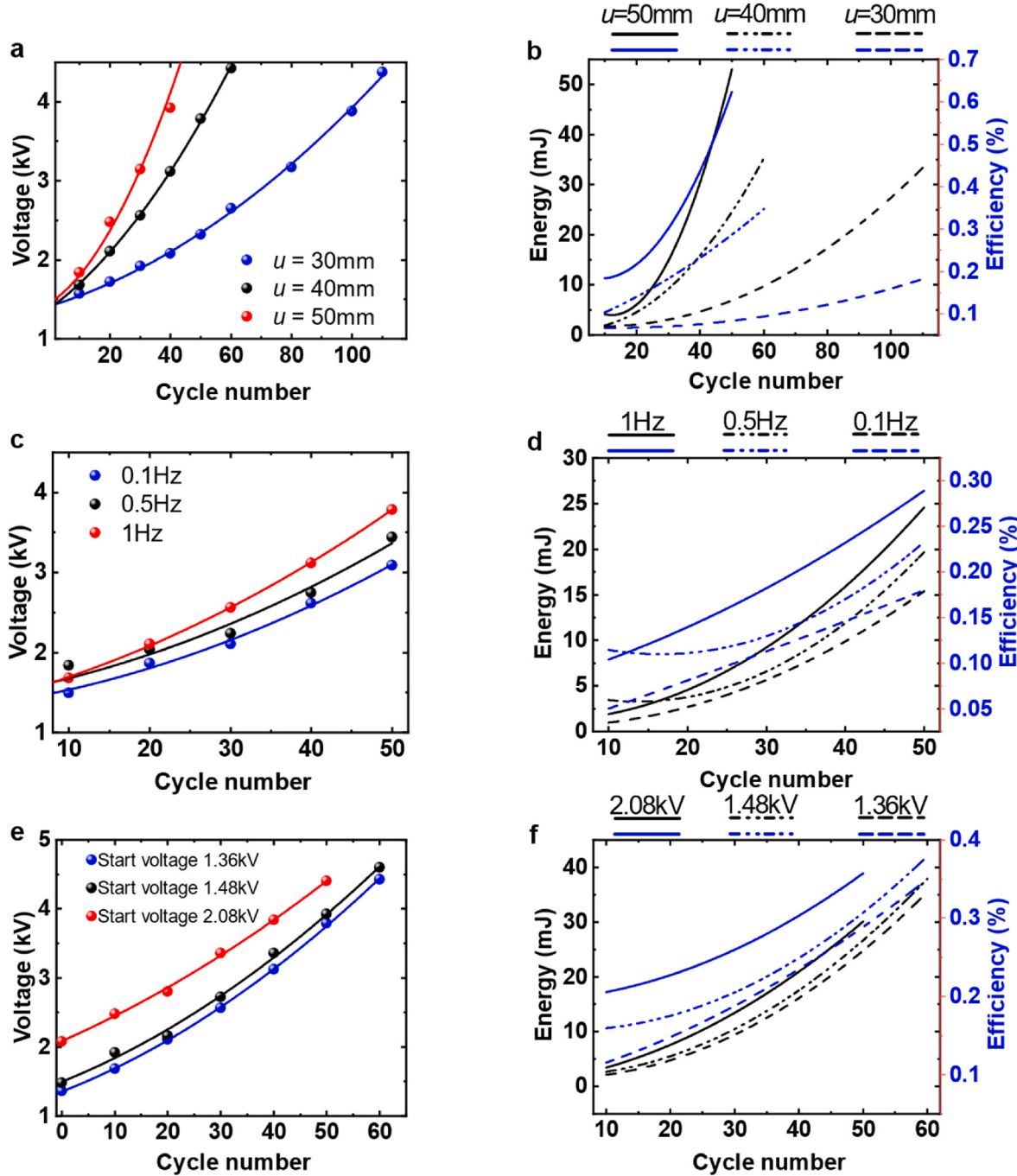


Fig. 12. Voltage boost and energy harvesting of the ODEG in multi cycles. (a–b) Voltage boost, harvested energy and efficiency in different displacement amplitude (start voltage: 1.4 kV; frequency: 1Hz); (c–d) Voltage boost, harvested energy and efficiency in different frequencies (start voltage: 1.4 kV; displacement amplitude: 40 mm); (e–f) Voltage boost, harvested energy and efficiency in different start voltage (displacement amplitude: 40 mm; frequency: 1Hz). (Note: the curves in the figure are second-order polynomial fit based on the experimental discrete points).

Validation, Methodology, Formal analysis, Data curation, Conceptualization. **Jinxin Wang:** Validation, Resources, Methodology, Data curation. **Tianyou Zhang:** Validation, Resources, Data curation. **Jung-Che Chang:** Methodology, Investigation. **Siqian Li:** Methodology, Conceptualization. **Yao Zhang:** Writing – review & editing, Supervision, Investigation, Conceptualization. **Tianyi Zeng:** Writing – review & editing, Supervision, Methodology, Investigation, Conceptualization. **Xin Dong:** Writing – review & editing, Supervision, Project administration, Investigation, Funding acquisition, Conceptualization.

Declaration of generative AI and AI-assisted technologies in the writing process

During the preparation of this work the authors used ChatGPT 4o to improve language and readability. After using this tool/service, the authors reviewed and edited the content as needed and take full

responsibility for the content of the publication.

Declaration of competing interest

The authors declare that they have no known competing financial interests or personal relationships that could have appeared to influence the work reported in this paper.

Acknowledgements

This work was supported by the China Scholarship Council Research Excellence Scholarship with the University of Nottingham (Dr Xi Wang, Mr Siqian Li, Mr Jinxin Wang), EPSRC (EP/W001128/1), Innovate UK (51689) and Wave Energy Scotland Direct Generation Competition Award.

Nomenclature

λ_1	radial strain of the elastomer
λ_2	circular strain of the elastomer
λ_3	strain of the elastomer in thickness
λ_p	pre-stretch ratio of the elastomer
r_o	original outer radius of the elastomer
r_i	original inner radius of the elastomer
h	original thickness of the elastomer
u	the displacement out-of-plane
F	external force to the ODEG
J_1	stretch limit of the elastomer
μ_1	shear modulus of the elastomer
W_s	energy density of the elastomer
\emptyset	applied voltage on the elastomer
D	area charge density
Q	electric charge
ϵ	the permittivity of the elastomer
σ_1	stress of the elastomer in radial direction
σ_2	stress of the elastomer in circular direction
E	electric strength
A	area of the deformed elastomer
W_m	input mechanical energy to the ODEG
W_{eh}	harvested energy from ODEG
W_{ei}	input electrical energy to the ODEG
\emptyset_B	voltage on the ODEG at State B
\emptyset_C	voltage on the ODEG at State C
C_B	capacitance of the ODEG at State B
C_C	capacitance of the ODEG at State C
C_1	capacitor in self-priming circuit
C_2	capacitor in self-priming circuit
C_{store}	capacitance of the storage capacitor
$C_{B_critical}$	the critical capacitance of the ODEG that triggers the self-priming circuit to switch between the high-voltage and high-charge states
C_{sp_hv}	capacitance of the self-priming circuit in high voltage state
C_{sp_hc}	capacitance of the self-priming circuit in high charge state
β	ratio of the capacitance between ODEG state B and state C
η	efficiency of the ODEG

References

- Abu Husain, M.K., Mohd Zaki, N.I., Che Husin, S.M., Mukhlis, N.A., Ahmad, R., Adanan, A.F., Ahmad Sukri, I.A., Husain, N.A.H., 2020. Wave energy converter using electromagnetic induction. *Int. J. Adv. Res. Eng. Technol.* 11 (9).
- Aubry, J., Ahmed, H.B., Multon, B., Babarit, A., Clément, A.H., 2011. Wave energy converters. *Marine Renewable Energy Handbook*.
- Binh, P.C., Ahn, K.K., 2016. Performance optimization of dielectric electro active polymers in wave energy converter application. *Int. J. Precis. Eng. Manuf.* 17, 1175–1185.
- Bortot, E., Gei, M., 2015. Harvesting energy with load-driven dielectric elastomer annular membranes deforming out-of-plane. *Extreme Mech. Lett.* 5, 62–73.
- Cao, J., Lu, G., Shiju, E., Gao, Z., Zhao, T., Xia, W., 2021. Electrostatic model of dielectric elastomer generator based on finite element. *Sci. Rep.* 11 (1), 14764.
- Chen, P., Wu, D., 2024. A review of hybrid wave-tidal energy conversion technology. *Ocean Eng.* 303, 117684.
- De Marinis, F., 2024. Advancements in Wave Energy Conversion: A Numerical Analysis of the C4 CorPower WEC's Dynamic Response in Various Wave Scenarios. *Politecnico di Torino*.
- Falcão, A.F., Henriques, J.C., 2016. Oscillating-water-column wave energy converters and air turbines: a review. *Renew. Energy* 85, 1391–1424.
- Fang, S., Wang, S., Zhang, G., Wang, C., Xu, J., Wang, Z., Feng, A., Qiao, Z., Yurchenko, D., Lai, Z., 2023. On high-performance rotational energy harvesting with a novel cam-like dielectric elastomer generator. *Sci. China Technol. Sci.* 66 (5), 1317–1334.
- Gu, G.-Y., Gupta, U., Zhu, J., Zhu, L.-M., Zhu, X., 2017. Modeling of viscoelastic electromechanical behavior in a soft dielectric elastomer actuator. *IEEE Trans. Robot.* 33 (5), 1263–1271.
- Gurjar, K.V.S., Sadangi, A.S., Kumar, A., Ahmad, D., Patra, K., Collins, I., Hossain, M., Ajaj, R.M., Zweiri, Y., 2025. Dielectric elastomer generators: recent advances in materials, electronic circuits, and prototype developments. *Adv. Energy Sustain. Res.* 6 (1), 2400221.

- Illeberger, P., Takagi, K., Kojima, H., Madawala, U.K., Anderson, I.A., 2016. A mathematical model for self-priming circuits: getting the most from a dielectric elastomer generator. *IEEE Trans. Power Electron.* 32 (9), 6904–6912.
- Illeberger, P.K., Rosset, S., Madawala, U.K., Anderson, I.A., 2020. The integrated self priming circuit: an autonomous electrostatic energy harvester with voltage boosting. *IEEE Trans. Ind. Electron.* 68 (8), 6982–6991.
- Jean-Mistral, C., Vu-Cong, T., Sylvestre, A., 2013. On the power management and electret hybridization of dielectric elastomer generators. *Smart Mater. Struct.* 22 (10), 104017.
- Ji, F., Wu, D., Li, Y., Zhu, Z., Zhu, L., 2021. Research on buoy-chain-sprocket wave energy capture technology. *Ocean Eng.* 235, 109397.
- Jiang, X., Xie, B., Bao, Y., Song, Z., 2023. Global 3-hourly wind-wave and swell data for wave climate and wave energy resource research from 1950 to 2100. *Sci. Data* 10 (1), 225.
- Jiang, Y., Liu, S., Zhong, M., Zhang, L., Ning, N., Tian, M., 2020. Optimizing energy harvesting performance of cone dielectric elastomer generator based on VHB elastomer. *Nano Energy* 71, 104606.
- Joensen, B., Bingham, H.B., 2024. Economic feasibility study for wave energy conversion device deployment in Faroese waters. *Energy* 295, 130869.
- Jusoh, M.A., Ibrahim, M.Z., Daud, M.Z., Albani, A., Mohd Yusop, Z., 2019. Hydraulic power take-off concepts for wave energy conversion system: a review. *Energies* 12 (23), 4510.
- Lai, Z., Xu, J., Fang, S., Qiao, Z., Wang, S., Wang, C., Huang, Z., Zhou, S., 2023. Energy harvesting from a hybrid piezo-dielectric vibration energy harvester with a self-priming circuit. *Energy* 273, 127205.
- Lv, X., Liu, L., Liu, Y., Leng, J., 2015. Dielectric elastomer energy harvesting: maximal converted energy, viscoelastic dissipation and a wave power generator. *Smart Mater. Struct.* 24 (11), 115036.
- McKay, T., O'Brien, B., Calius, E., Anderson, I., 2010. Self-priming dielectric elastomer generators. *Smart Mater. Struct.* 19 (5), 055025.
- McKay, T.G., Rosset, S., Anderson, I.A., Shea, H., 2014. Dielectric elastomer generators that stack up. *Smart Mater. Struct.* 24 (1), 015014.
- Medina, H., Farmer, C., Liu, I., 2024. Dielectric Elastomer-Based Actuators: A Modeling and Control Review for Non-experts. *Actuators*. MDPI, p. 151.
- Moretti, G., Fontana, M., Vertechy, R., 2015. Model-based design and optimization of a dielectric elastomer power take-off for oscillating wave surge energy converters. *Meccanica* 50, 2797–2813.
- Moretti, G., Herran, M.S., Forehand, D., Alves, M., Jeffrey, H., Vertechy, R., Fontana, M., 2020a. Advances in the development of dielectric elastomer generators for wave energy conversion. *Renew. Sustain. Energy Rev.* 117, 109430.
- Moretti, G., Malara, G., Scialò, A., Daniele, L., Romolo, A., Vertechy, R., Fontana, M., Arena, F., 2020b. Modelling and field testing of a breakwater-integrated U-OWC wave energy converter with dielectric elastomer generator. *Renew. Energy* 146, 628–642.
- Moretti, G., Rosati Papini, G.P., Daniele, L., Forehand, D., Ingram, D., Vertechy, R., Fontana, M., 2019. Modelling and testing of a wave energy converter based on dielectric elastomer generators. *Proceed. Royal Soc. Aedings of the Royal Society A* 475 (2222), 20180566.
- Moretti, G., Rosset, S., Vertechy, R., Anderson, I., Fontana, M., 2020c. A review of dielectric elastomer generator systems. *Adv. Intell. Sys.* 2 (10), 30.
- Renzi, E., 2016. Hydroelectromechanical modelling of a piezoelectric wave energy converter. *Proc. R. Soc. A* 472 (2195), 20160715.
- Sergienko, N.Y., Cannard, P.A., Cui, L., Leontini, J.S., Manasseh, R., Cazzolato, B., 2024. Impact of wave energy converters on infragravity waves: an experimental investigation. *Ocean Eng.* 309, 118345.
- Song, Z.-Q., Ohyama, K., Shian, S., Clarke, D.R., Zhu, S., 2019. Power generation performance of dielectric elastomer generator with laterally-constrained configuration. *Smart Mater. Struct.* 29 (1), 015018.
- Srivastava, A.K., Basu, S., 2021. Exploring the performance of a dielectric elastomer generator through numerical simulations. *Sensor Actuator Phys.* 319, 112401.
- Vertechy, R., Papini Rosati, G.P., Fontana, M., 2015. Reduced model and application of inflating circular diaphragm dielectric elastomer generators for wave energy harvesting. *J. Vib. Acoust.* 137 (1), 011004.
- Viet, N., Wang, Q., 2018. Ocean wave energy pitching harvester with a frequency tuning capability. *Energy* 162, 603–617.
- Wang, X., Li, S., Chang, J.-C., Liu, J., Axinte, D., Dong, X., 2024a. Multimodal locomotion ultra-thin soft robots for exploration of narrow spaces. *Nat. Commun.* 15 (1), 6296.
- Wang, X., Raimondi, L., Axinte, D., Dong, X., 2024b. Investigation on a class of 2D profile amplified stroke dielectric elastomer actuators. *J. Mech. Robot.* 1–32.
- Xiao, H., Liu, Z., Zhang, R., Kelham, A., Xu, X., Wang, X., 2021. Study of a novel rotational speed amplified dual turbine wheel wave energy converter. *Appl. Energy* 301, 117423.
- Zeng, F., Wang, T., 2023. In-situ wave energy harvesting for unmanned marine devices: a review. *Ocean Eng.* 285, 115376.
- Zhang, J., 2022. Rotational energy harvesting from a novel arc-cylinder type vibro-impact dielectric elastomer generator. *Int. J. Mech. Mater. Des.* 18 (3), 587–609.
- Zhou, T., 2016. Damping Profile Research for CorPower Ocean's Wave Energy Converter.